Please cite this article in press as: Tatebe et al., Pom1 DYRK Regulates Localization of the Rga4 GAP to Ensure Bipolar Activation of Cdc42 in Fission Yeast, Current Biology (2008), doi:10.1016/j.cub.2008.02.005

Supplemental Data

Pom1 DYRK Regulates Localization of the Rga4 GAP to Ensure Bipolar Activation of Cdc42 in Fission Yeast

Hisashi Tatebe, Kentaro Nakano, Rachel Maximo, and Kazuhiro Shiozaki

Supplemental Experimental Procedures

Yeast Two-Hybrid Screens

The entire open reading frame (ORF) of *pom1*$^+$ was cloned in the pGBT9 vector (Clontech) to express the *GAL4* DNA-binding domain fused to the Pom1 protein. By using a *S. pombe* cDNA library constructed in the pGADGH vector (Clontech) and the budding yeast strain HF7c [S1], approximately 2.4 × 10^7 transformants were screened by histidine auxotrophy and β-galactosidase assay. Library plasmids were recovered from positive yeast transformants and verified for expression of the reporter genes by retransformation, followed by DNA sequencing and/or Southern hybridization.

Interaction between Pom1 and Rga4 was further characterized by yeast two-hybrid assays. The partial fragments of Rga4 fused to the *GAL4* transcription activation domain were expressed from pGADGH. The full-length and partial fragments Pom1 fused to the *GAL4* DNA-binding domain were expressed from pGBT9. By using the budding yeast HF7c strain, histidine-dependent growth was examined either in the absence or in the presence of varied concentrations (1–8 mM) of 3-amino-1,2,4-triazole (3-AT), an inhibitor of histidine biosynthesis.

Cell Lysate Preparation and Immunoprecipitation

Harvested cells were disrupted by vigorous vortexing for 5 min at 4°C with 0.5 mm diameter glass beads in lysis buffer A (1× PBS, 0.5% Tween-20, 10 mM p-nitrophenylphosphate, 10 mM sodiumpyrophosphate, 10 mM β-glycerophosphate, 0.1 mM Na_3VO_4, 1 mM phenylmethylsulfonyl fluoride, and protease inhibitor cocktail [P8215, Sigma]), and cleared by centrifugation at 2300 × g for 10 min [S2]. The supernatant was incubated at 4°C for 2 hr with anti-FLAG M2 affinity gel (Sigma), followed by extensive washes with the lysis buffer. The lysate and immunoprecipitates were analyzed by immunoblotting with anti-FLAG antibodies (M2, Sigma) and anti-*myc* antibodies (A14, Santa Cruz).

For the lysate fractionation experiments, cells were disrupted by glass beads at 4°C in lysis buffer B (20 mM Tris-HCl [pH 7.5], 150 mM NaCl, 0.5% Tween-20, 1 mM phenylmethylsulfonyl fluoride, leupeptin, and aprotinin). Total cell homogenate and the supernatant after centrifugation at 2300 × g for 5 min was analyzed by SDS-PAGE followed by anti-FLAG and anti-Spc1 immunoblotting. Preparation of TCA-denatured crude lysate for immunoblotting analysis was performed as described previously [S3].

λ Protein Phosphatase Treatment

Three microliters of TCA-denatured crude lysate [S3] was incubated at 30°C for 30 min in 60 μl of 1× λ protein phosphatase buffer containing 80 U of λ protein phosphatase (New England BioLabs), 2 mM $MnCl_2$, and 1% Triton X-100. As a negative control experiment, phosphatase treatment was performed in the phosphatase buffer without $MnCl_2$ in the presence of the phosphatase inhibitor cocktail (10 mM NaVO4, 50 mM NaF, 50 mM β-glycerophosphate, 20 mM *p*-nitrophenylphosphate, and 50 mM EDTA [pH 8.0]).

Interaction of Rga4 with Cdc42

For yeast two-hybrid interaction assays of the Rga4 RhoGAP domain, a budding yeast strain, L40, was transformed with a pBTM116-based plasmid carrying the Rga4 RhoGAP domain (745–933 aa). The resultant transformant was then transformed with pCAD422 carrying either wild-type or GTP-locked mutants of Cdc42, Rho1, Rho3, and Rho4. GTP-locked mutants used were Cdc42Q61L, Rho1Q64L, Rho3Q71L, and Rho4Q74L. To prevent the lipid modification at the C terminus, the C-terminal cysteine residue in each Rho GTPase was substituted with serine (Cdc42C189S, Rho1C199S, Rho3C202S, and Rho4C200S). Interaction was determined by histidine auxotrophy.

For the in vitro interaction assay, *S. pombe cdc42*$^+$ cDNA was cloned in pGEX-KG [S4] and the Q61L mutation was introduced with the QuikChange kit (Stratagene) to express the GTP-locked mutant protein [S5]. The GST-Cdc42 and GST-Cdc42Q61L proteins were expressed in *E. coli* DH5α strain and absorbed onto glutathione-Sepharose 4B (Amersham) [S5]. Cell lysate of strain CA4462 was prepared in lysis buffer B and incubated with the GST-Cdc42 beads at 4°C for 1 hr in the presence of 5 mM $MgCl_2$. The Rga4FLAG protein bound to the beads was detected by anti-FLAG immunoblotting.

Detection of GTP-Bound Cdc42

The procedure reported by Benard et al. [S6] was adopted. The CRIB domain of *S. pombe* Shk1 (residues 135–227) was expressed in *E. coli* DH5α as a GST-fusion protein by using the pGEX-KG vector [S4]. The GTP-bound HA-Cdc42 protein precipitated by the GST-CRIB beads was detected by anti-HA (12CA5, Boehringer) immunoblotting.

Isolation of *cdc42*^{ts} Mutants

The PCR-based method described by Uritani et al. [S7] was used with modifications to introduce mutations to the *S. pombe cdc42*$^+$ locus. The details will be published elsewhere. Briefly, the *kanMX6* marker cassette was integrated downstream of the *cdc42*$^+$ ORF, and the genomic DNA from the resultant strain was used as template in PCR to amplify the *cdc42*$^+$ locus and the downstream *kanMX6* marker gene. The amplified DNA fragment was used to transform a wild-type strain, and G418-resistant, temperature-sensitive (*ts*) transformants were isolated. Genomic sequencing confirmed missense mutations in the *cdc42* ORF. The *ts* phenotypes of both *cdc42-2* and *cdc42-3* mutants were complemented by a plasmid carrying the wild-type *cdc42*$^+$ gene (data not shown).

Construction of the *rga4R783G* Mutant

Site-directed mutagenesis was conducted by using the QuikChange kit (Stratagene) with the following oligoDNA primers: rga4_2668-712_C89G, 5′-ATGGATTTTGAAGGTCTGTATGGCAAGAGCGGGGCAACTTCTCAA-3′; and rga4_2712-2668_C89, 5′-TTGAGAAGTTGCCCCGCTCTTGCCATACAG ACCTTCAAAATCCAT-3′. Underlined letters indicate nucleotides changed in mutagenesis. Substitution from arginine to glycine at the 783rd amino acid position in *rga4* was confirmed by DNA sequencing.

Microscopy

To observe Rga4-GFP in *cdc10-V50* mutant, cells grown in liquid EMM at the permissive temperature (25°C) were mounted and immobilized on thin EMM (agarose film under coverslip). After sealing coverslip, *cdc10* mutant cells were incubated for 4 hr in the dark at the restrictive temperature (36°C). In this experimental condition, *cdc10* cells divided once and arrested in G1 phase before NETO [S8], forming pairs of daughter cells.

Supplemental References

S1. Feilotter, H.E., Hannon, G.J., Ruddell, C.J., and Beach, D. (1994). Construction of an improved host strain for two hybrid screening. Nucleic Acids Res. *22*, 1502–1503.

S2. Urano, J., Comiso, M.J., Guo, L., Aspuria, P.J., Deniskin, R., Tabancay, A.P., Jr., Kato-Stankiewicz, J., and Tamanoi, F. (2005). Identification of novel single amino acid changes that result in hyperactivation of the unique GTPase, Rheb, in fission yeast. Mol. Microbiol. *58*, 1074–1086.

S3. Tatebe, H., and Shiozaki, K. (2003). Identification of Cdc37 as a novel regulator of the stress-responsive mitogen-activated protein kinase. Mol. Cell. Biol. *23*, 5132–5142.

S4. Guan, K.L., and Dixon, J.E. (1991). Eukaryotic proteins expressed in Escherichia coli: An improved thrombin cleavage and purification procedure of fusion proteins with glutathione S-transferase. Anal. Biochem. *192*, 262–267.

S5. Garcia-Mata, R., Wennerberg, K., Arthur, W.T., Noren, N.K., Ellerbroek, S.M., and Burridge, K. (2006). Analysis of activated GAPs and GEFs in cell lysates. Methods Enzymol. *406*, 425–437.

S6. Benard, V., Bohl, B.P., and Bokoch, G.M. (1999). Characterization of rac and cdc42 activation in chemoattractant-stimulated human neutrophils using a novel assay for active GTPases. J. Biol. Chem. *274*, 13198–13204.

Please cite this article in press as: Tatebe et al., Pom1 DYRK Regulates Localization of the Rga4 GAP to Ensure Bipolar Activation of Cdc42 in Fission Yeast, Current Biology (2008), doi:10.1016/j.cub.2008.02.005

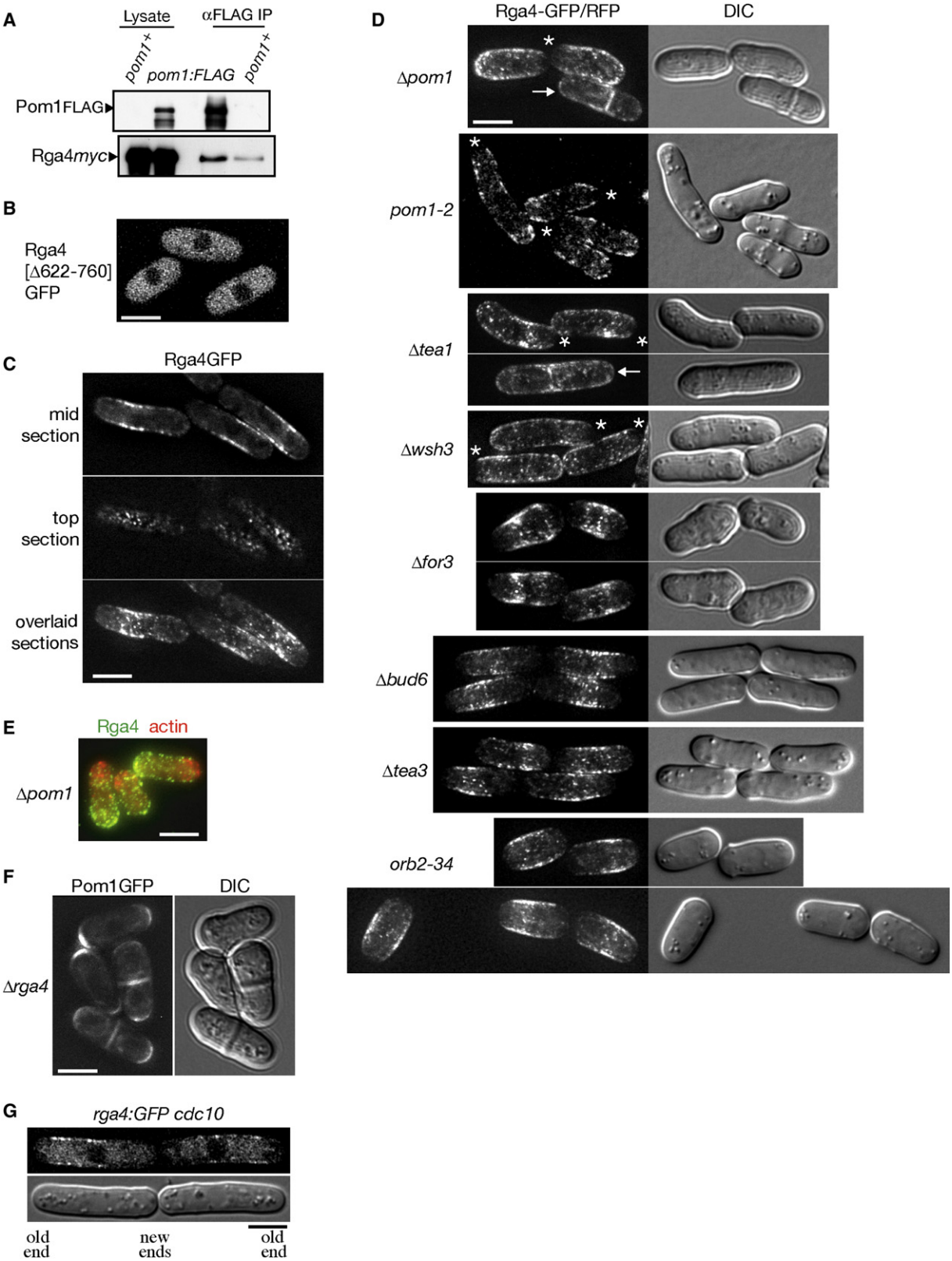

Figure S1. Cellular Localization of Rga4 Is Regulated by Pom1 Kinase at Cell Ends

(A) Rga4 is copurified with Pom1. Anti-FLAG immunoprecipitation was performed as in Figure 1B with *rga4:myc* strains carrying the untagged *pom1*$^{+}$ (CA4466) or *pom1:FLAG* (CA5156) alleles, followed by immunoblotting with anti-FLAG and anti-*myc* antibodies.

(B) Residues 622–760 are required for cortical localization of Rga4. A strain was constructed in which the GFP-fused Rga4 mutant lacking residues 622–760 was expressed under the native promoter from the *rga4* locus (CA5544). The resultant strain was observed under fluorescence microscopy. Immunoblotting

S7. Uritani, M., Hidaka, H., Hotta, Y., Ueno, M., Ushimaru, T., and Toda, T. (2006). Fission yeast Tor2 links nitrogen signals to cell proliferation and acts downstream of the Rheb GTPase. Genes Cells *11*, 1367–1379.
S8. Mitchison, J.M., and Nurse, P. (1985). Growth in cell length in the fission yeast Schizosaccharomyces pombe. J. Cell Sci. *75*, 357–376.
S9. Thompson, J.D., Higgins, D.G., and Gibson, T.J. (1994). CLUSTAL W: Improving the sensitivity of progressive multiple sequence alignment through sequence weighting, position-specific gap penalties and weight matrix choice. Nucleic Acids Res. *22*, 4673–4680.
S10. Clamp, M., Cuff, J., Searle, S.M., and Barton, G.J. (2004). The Jalview Java alignment editor. Bioinformatics *20*, 426–427.
S11. Bähler, J., and Pringle, J.R. (1998). Pom1p, a fission yeast protein kinase that provides positional information for both polarized growth and cytokinesis. Genes Dev. *12*, 1356–1370.
S12. Mata, J., and Nurse, P. (1997). tea1 and the microtubular cytoskeleton are important for generating global spatial order within the fission yeast cell. Cell *89*, 939–949.
S13. Bähler, J., and Nurse, P. (2001). Fission yeast Pom1p kinase activity is cell cycle regulated and essential for cellular symmetry during growth and division. EMBO J. *20*, 1064–1073.
S14. Glynn, J.M., Lustig, R.J., Berlin, A., and Chang, F. (2001). Role of bud6p and tea1p in the interaction between actin and microtubules for the establishment of cell polarity in fission yeast. Curr. Biol. *11*, 836–845.
S15. Nakano, K., Mutoh, T., and Mabuchi, I. (2001). Characterization of GTPase-activating proteins for the function of the Rho-family small GTPases in the fission yeast Schizosaccharomyces pombe. Genes Cells *6*, 1031–1042.
S16. Hirota, K., Tanaka, K., Ohta, K., and Yamamoto, M. (2003). Gef1p and Scd1p, the Two GDP-GTP exchange factors for Cdc42p, form a ring structure that shrinks during cytokinesis in Schizosaccharomyces pombe. Mol. Biol. Cell *14*, 3617–3627.
S17. Verde, F., Mata, J., and Nurse, P. (1995). Fission yeast cell morphogenesis: Identification of new genes and analysis of their role during the cell cycle. J. Cell Biol. *131*, 1529–1538.
S18. Nakano, K., Imai, J., Arai, R., Toh, E.A., Matsui, Y., and Mabuchi, I. (2002). The small GTPase Rho3 and the diaphanous/formin For3 function in polarized cell growth in fission yeast. J. Cell Sci. *115*, 4629–4639.

confirmed that the mutant Rga4 protein was expressed at a level similar to that of wild-type Rga4 (data not shown).
(C) Fluorescence microscopy of a wild-type strain carrying the *rga4:GFP* allele (CA4699). Z-axial images were taken at 0.4 μm steps and deconvolved. 'mid section' and 'top section' represent a single focal plane at the middle of cells and at the top surface of cells, respectively.
(D) The *Δpom1*, *pom1-2*, *Δtea1*, and *Δwsh3* mutants show a "sock"-like localization pattern of Rga4. Rga4GFP or Rga4RFP was observed under fluorescence microscopy in *Δpom1* (CA4707), *pom1-2* (CA5913), *Δtea1* (CA4713), *Δwsh3* (CA4717), *Δfor3* (CA4710), *Δbud6* (CA6084), *Δtea3* (CA6085), and *orb2-34* (CA6095) mutants. Projection images were composed by stacking Z-axial images after deconvolution. Asterisks mark the cell ends from which Rga4GFP was excluded. Arrows indicate dividing cells.
(E) Rga4 is not excluded from the non-growing end of *Δpom1* cells. *Δpom1* cells expressing Rga4GFP (CA4707) were grown in YES medium and fixed in formaldehyde. F-actin and Rga4 were visualized with rhodamine-phalloidin and anti-GFP antibodies, respectively. Fluorescence images were pseudo colored (F-actin, red; Rga4GFP, green) and superimposed.
(F) Pom1 is localized at cell ends of the *Δrga4* mutant. Images of a *Δrga4* strain carrying the *pom1:GFP* allele (CA4168) were taken by fluorescence and DIC microscopy.
(G) Rga4 is excluded from both cell ends in G1-arrested cells. A *cdc10-V50* strain carrying the *rga4:GFP* allele (CA5225) was incubated at 36°C for 4 hr before fluorescence microscopy. Z-axial images were taken, deconvolved, and stacked. Rga4 remains excluded from both cell ends while the mutant cells grow only at the old cell end.
Scale bars represent 5 μm.

Please cite this article in press as: Tatebe et al., Pom1 DYRK Regulates Localization of the Rga4 GAP to Ensure Bipolar Activation of Cdc42 in Fission Yeast, Current Biology (2008), doi:10.1016/j.cub.2008.02.005

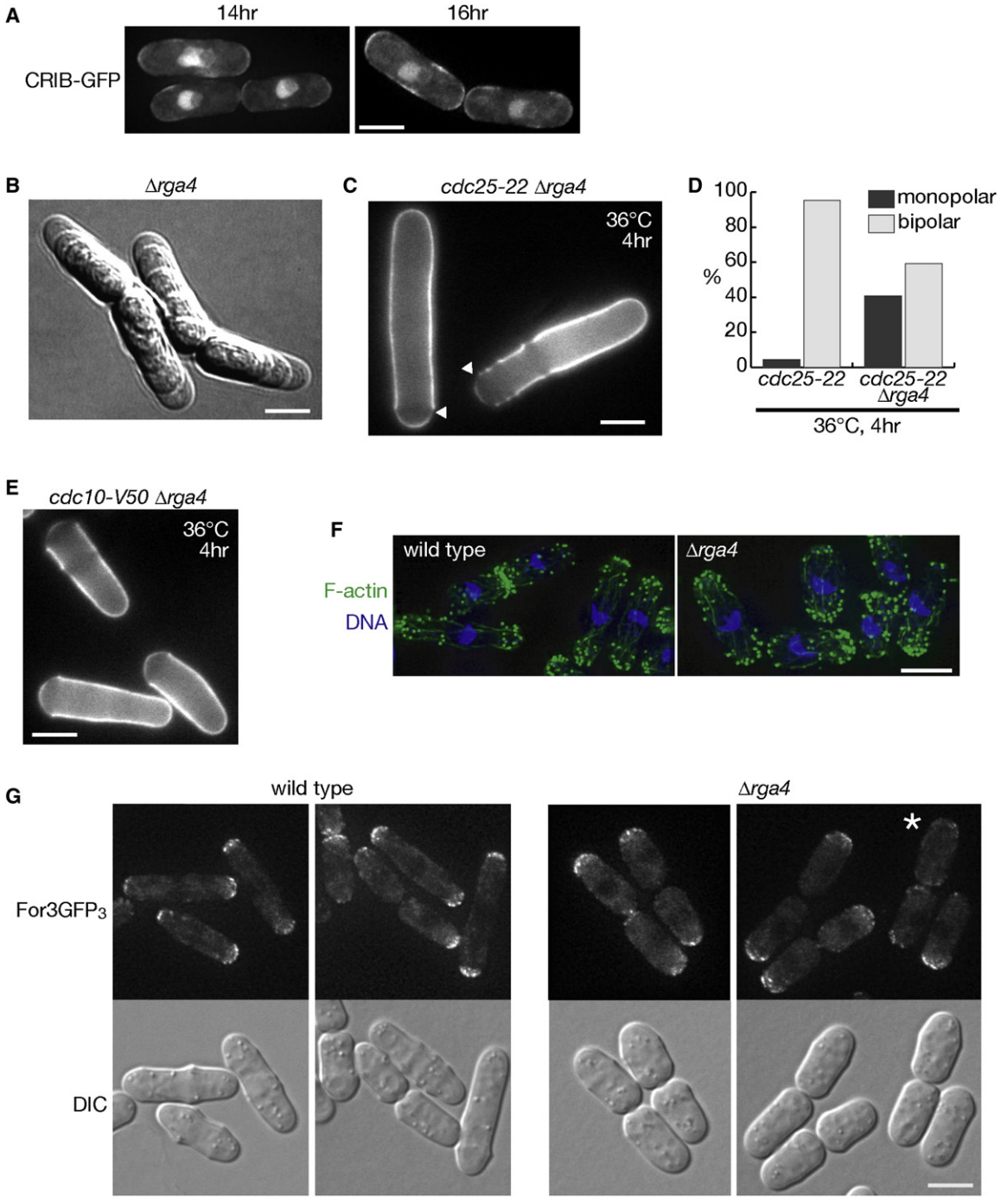

Figure S2. The *Δrga4* Mutant Is Defective in NETO

(A) CRIB-GFP distribution is affected by ectopic overexpression of Pom1. CRIB-GFP images of the cells presented in Figure 2C. Under this experimental condition, both CRIB-GFP and Rga4RFP (Figure 2C) were often detectable at cell tips.

(B) *Δrga4* cells grow only at the old end when mounted between cover glass and solid agarose medium. *Δrga4* cells (CA4168) were mounted on EMM agarose under cover glass. Cell growth at room temperature (28–30°C) was monitored under DIC microscopy for 335 min, and the five time-course images at 40 min intervals were superimposed. Similar results were obtained in 14 *Δrga4* mutant cells.

(C and D) The *Δrga4* mutant is partially defective in NETO. *cdc25-22* (CA2302) and *cdc25-22 Δrga4* (CA4230) strains grown in YES at 25°C were shifted to 36°C for 4 hr before Calcofluor staining. The temperature-sensitive *cdc25-22* mutant arrests in G2 after NETO with continued bipolar growth [S8]. In contrast, 41% of the double mutant cells were found to continue monopolar growth at the old end even after the cell cycle arrest, leaving a weakly stained birth scar at the new end. Arrowheads indicate birth scars formed in the previous cell division. ≥200 cells from each strain were analyzed for their growth pattern and shown in the graph.

(E) The *Δrga4* mutant initiates growth from the old end after cell division. *cdc10-V50 Δrga4* cells (CA4233) were incubated in YES medium at 36°C for 4 hr to induce cell cycle arrest in G1 before NETO and fixed for Calcofluor staining. 96% (n = 213) of the double mutant cells grew exclusively at the old end, with the birth scar remaining at the new end.

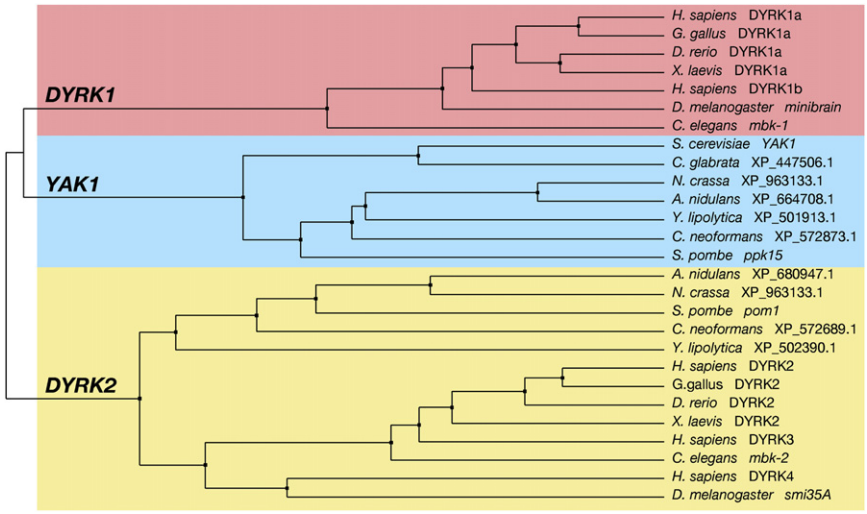

Figure S3. A Phylogenetic Tree for the Kinase Domain Sequences of DYRKs from Fungi, Invertebrates, and Vertebrates

The phylogenetic tree was built by using the ClustalW software [S9] and the JalView software [S10]. The kinases included are: Q13627 (*H. sapiens* DYRK1a, Swiss-Prot), Q9Y463 (*H. sapiens* DYRK1b, Swiss-Prot), Q92630 (*H. sapiens* DYRK2, Swiss-Prot), O43781 (*H. sapiens* DYRK3, Swiss-Prot), Q9NR20 (*H. sapiens* DYRK4, Swiss-Prot), AAF53380.1 (*D. melanogaster smi35A*, GenBank), P49657 (*D. melanogaster* minibrain, Swiss-Prot), Q8WQL7 (*C.elegans mbk-1*, Swiss-Prot), Q9TVF4 (*C.elegans mbk-2*, Swiss-Prot), *S. cerevisiae YAK1* (GeneDB), *S. pombe pom1* (GeneDB), *S. pombe ppk15* (GeneDB), XP_680947.1 (*A. nidulans*, GenBank), XP_963133.1 (*N. crassa,* GenBank), XP_960871.1 (*N. crassa,* GenBank), XP_502390.1 (*Y. lipolytica*, GenBank), XP_572873.1 (*C. neoformans*, GenBank), XP_664708.1 (*A. nidulans*, GenBank), XP_501913.1 (*Y. lipolytica*, GenBank), XP_447506.1 (*C. glabrata*, GenBank), XP_572689.1 (*C. neoformans*, GenBank), NP_001026651.1 (*G. gallus* DYRK2, GenBank), XP_683531.1 (*D. rerio* DYRK2, GenBank), NP_989881.1 (*G. gallus* DYRK1a, GenBank), XP_684056.2 (*D. rerio* DYRK1a, GenBank), AAH87464.1 (*X. laevis* DYRK2, GenBank), AAH44104.1, and (*X. laevis* DYRK1a, GenBank). The kinase domain was defined according to the Pfam database entry (PF00069).

(F) F-actin structures in wild-type and *Δrga4* cells. Wild-type (KNW441) and *Δrga4* (KNG401) strains grown in YES medium were fixed and stained for F-actin with bodipy-phalloidin. Z-axial images were taken and projected after deconvolution.

(G) Fluorescence microscopy of wild-type (CA5818) and *Δrga4* (CA5815) strains carrying the *for3:GFP3* allele. Z-axial images were take at 0.4 μm steps and deconvolved for projection images. An asterisk indicates a *Δrga4* cell in which For3 localization was not clearly polarized.

Scale bars represent 5 μm.

Please cite this article in press as: Tatebe et al., Pom1 DYRK Regulates Localization of the Rga4 GAP to Ensure Bipolar Activation of Cdc42 in Fission Yeast, Current Biology (2008), doi:10.1016/j.cub.2008.02.005

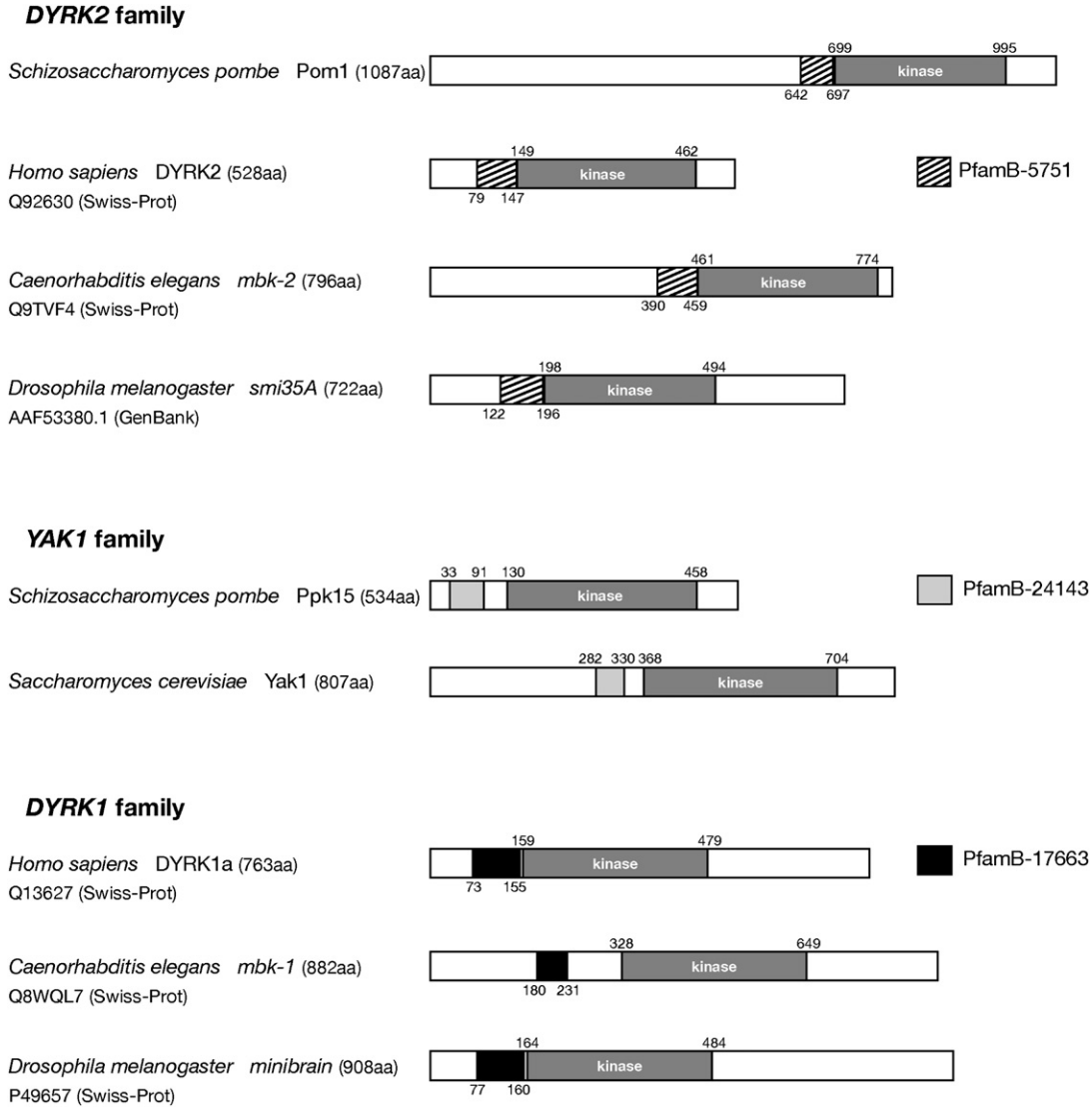

Figure S4. Primary Structures of Members in the DYRK Subfamilies

Representatives of the three DYRK subfamilies were chosen from human, fly, worm, budding yeast, and fission yeast. The kinase domain was defined according to the Pfam database entry (PF00069). In addition to the kinase domain, members of the DYRK subfamilies share a conserved region unique to each subfamily: PfamB-5751 (PB005751) for the DYRK2 subfamily, PfamB-17663 (PB017663) for the DYRK1 subfamily, and PfamB-24143 (PB024143) for the YAK1 subfamily. Numbers indicate positions in amino acid sequences.

Table S1. *S. pombe* Strains Used in This Study

Strain	Genotype	Source or Reference
CA3	*ura4-D18*	Lab stock
CA2302	*ura4-D18 cdc25-22*	Lab stock
CA2520	*ura4-D18 pom1:GFP(kanMX6)*	[S11]
CA2529	*ura4-D18 cdc10-V50*	Lab stock
CA2548	*ura4-D18 Δtea1::ura4+*	[S12]
CA3125	*ura4-D18 pom1-2:GFP(kanMX6)*	[S13]
CA3252	*leu1+ Δbud6::kanMX6*	[S14]
CA3333	*ura4-D18 Δpom1::ura4+*	[S11]
CA4166	*ura4-D18 Δrga4::ura4+*	[S15]
CA4168	*ura4-D18 pom1:GFP(kanMX6) Δrga4::ura4+*	This study
CA4230	*ura4-D18 cdc25-22 Δrga4::ura4+*	This study
CA4233	*ura4-D18 cdc10-V50 pom1:GFP(kanMX6) Δrga4::ura4+*	This study
CA4462	*ura4-D18 rga4:3FLAG(kanMX6)*	This study
CA4466	*ura4-D18 rga4:12myc(kanMX6)*	This study
CA4496	*ura4-D18 rga4:3FLAG(kanMX6) Δpom1::ura4+*	This study
CA4628	*h90 ura4-D18 ade6-M216 Δscd1::ura4+*	[S16]
CA4699	*ura4-D18 rga4:GFP(kanMX6)*	This study
CA4707	*ura4-D18 rga4:GFP(kanMX6) Δpom1::ura4+*	This study
CA4710	*ura4-D18 rga4:GFP(kanMX6) Δfor3::ura4+*	This study
CA4713	*ura4-D18 rga4:GFP(kanMX6) Δtea1::ura4+*	This study
CA4717	*ura4-D18 rga4:GFP(kanMX6) Δwsh3::ura4+*	This study
CA4858	*ura4-D18 cdc42-3(kanMX6)*	This study
CA5128	*ura4-D18 pom1:13myc(kanMX6)*	This study
CA5156	*ura4-D18 pom1:3FLAG(kanMX6) rga4:12myc(kanMX6)*	This study
CA5188	*ura4-D18 nmt1:3HA:cdc42(kanMX6)*	This study
CA5225	*ura4-D18 cdc10-V50 rga4:GFP(kanMX6)*	This study
CA5544	*ura4-D18 rga4Δ622-760aa:GFP(ura4+)*	This study
CA5547	*ura4-D18 pom1:13myc(kanMX6) rga4:3FLAG(ura4+)*	This study
CA5815	*ura4-D18 for3:3GFP(kanMX6) Δrga4::ura4+*	This study
CA5818	*ura4-D18 for3:3GFP(kanMX6)*	This study
CA5911	*ura4-D18 pom1-2:GFP(kanMX6) rga4:3FLAG(kanMX6)*	This study
CA5913	*ura4-D18 pom1-2:GFP(kanMX6) rga4:RFP(kanMX6)*	This study
CA5929	*CRIB:GFP(ura4+) rga4:RFP(kanMX6)*	This study
CA5931	*CRIB:GFP(ura4+)*	This study
CA5932	*CRIB:GFP(ura4+) Δrga4::ura4+*	This study
CA5939	*CRIB:GFP(ura4+) Δscd1::ura4+*	This study
CA5949	*ura4-D18 Δtea1::ura4+ rga4:3FLAG(kanMX6)*	This study
CA6009	*CRIB:GFP(ura4+) Δpom1::ura4+ Δrga4::ura4+*	This study
CA6011	*CRIB:GFP(ura4+) Δpom1::ura4+ rga4:RFP(kanMX6)*	This study
CA6084	*ura4-D18 rga4:GFP(kanMX6) Δbud6::kanMX6*	This study
CA6085	*ura4-D18 rga4:GFP(kanMX6) Δtea3::kanMX6*	This study
CA6070	*ade6-M216 orb2-34*	[S17]
CA6095	*rga4:GFP(kanMX6) orb2-34*	This study
CA6165	*CRIB:GFP(ura4+) Δpom1::ura4+ rga4R783G:3FLAG(kanMX6)*	This study
KNF303	*h+ ura4-D18 ade6-M210 Δfor3::ura4+*	[S18]
KNG401	*ura4-D18 ade6-M216 Δrga4::ura4+*	[S15]
KNW441	*ade6-M216*	Lab stock

All strains are *h− leu1-32* unless indicated.